

## Original article

## Synthesis, Crystal Structure and the Effect of Iron Doped on Physical Properties of $\text{CaLaMn}_{1-x}\text{Fe}_x\text{TiO}_6$ ( $x= 0, 0.33$ and $0.67$ ) Double Perovskite

Maha A. Mohamad Ali<sup>1</sup>, Abdelrahman A. Elbadaw<sup>1,2\*</sup>, Yousef A. Alsabah<sup>1,3</sup>, Osama A. Yassen<sup>1,4</sup>

<sup>1</sup>Department of Physics, Faculty of Science and Technology, Al Neelain University, Khartoum, Sudan; <sup>2</sup>Research Chair in Laser Diagnosis of Cancers, College of Science, King Saud University, Riyadh, Kingdom of Saudi Arabia; <sup>3</sup>Department of Physics, Faculty of Education and Applied Science, Hajjah University, Hajjah, Yemen; <sup>4</sup>Department of Physics, College of Science, Taibha University, Almadina, Kingdom of Saudi Arabia.

## ARTICLE INFO

**Article history:**

Received 2018 April 10<sup>th</sup>

Reviewed 2018 October 20<sup>th</sup>

Accepted 2018 November 19<sup>th</sup>

**Keywords:**

Double Perovskite solar cell, x-ray diffraction, IV, UV, vis, space group. IV characteristic

**Abstract**

A new double perovskite compounds  $\text{CaLaMnTiO}_6$ ,  $\text{CaLaMn}_{0.67}\text{Fe}_{0.33}\text{TiO}_6$  and  $\text{CaLaMn}_{0.33}\text{Fe}_{0.67}\text{TiO}_6$  were prepared successfully using solid state reaction method to provide a solar cell. The X ray diffraction XRD, UV- visible spectroscopies were used to characterize the structural and optical properties of the synthesized compound. From X ray powder diffraction (XRD) examination, the samples show variation in structure from monoclinic structure with  $(P2_1/n)$  for  $\text{CaLaMnTiO}_6$  up to a cubic structure with  $(Pm-3m)$  space group for  $\text{CaLaMn}_{0.67}\text{Fe}_{0.33}\text{TiO}_6$  and  $\text{CaLaMn}_{0.33}\text{Fe}_{0.67}\text{TiO}_6$ , and the lattice parameters were investigated and found to be  $a = 5.47953 \text{ \AA}$ ,  $b = 5.54992 \text{ \AA}$ ,  $c = 7.76430 \text{ \AA}$  for  $\text{CaLaMnTiO}_6$ , and  $a = 3.9471, 3.868 \text{ \AA}$  for  $\text{CaLaMn}_{0.67}\text{Fe}_{0.33}\text{TiO}_6$  and  $\text{CaLaMn}_{0.33}\text{Fe}_{0.67}\text{TiO}_6$  respectively, where this varied result comes from the cation size disorder. The band gap energy was calculated; and found to be decreased from 5 to 3.6 eV for the series. The efficiency of the solar panel was measured via the current-voltage (I-V) characteristic curve, and the results were observed. The efficiency of the three samples was decreased from  $\eta = 1.18, 0.42$  and  $0.32 \%$  for  $\text{CaLaMnTiO}_6$ ,  $\text{CaLaMn}_{0.67}\text{Fe}_{0.33}\text{TiO}_6$  and  $\text{CaLaMn}_{0.33}\text{Fe}_{0.67}\text{TiO}_6$  respectively.

\*Corresponding author: [bahlaoy.ab@gmail.com](mailto:bahlaoy.ab@gmail.com)

**Introduction**

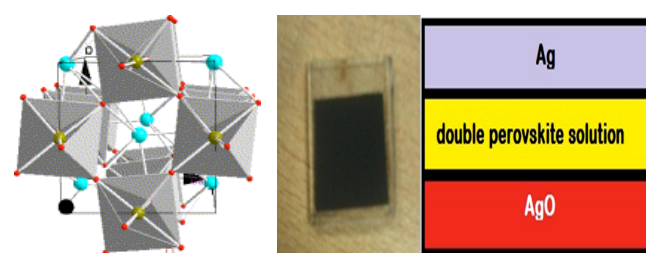
In 1839 The  $\text{CaTiO}_3$  mineral perovskite was discovered from samples obtained in the Ural Mountains. The first synthetic perovskite compounds were produced by Goldschmid (1926) of the University of Oslo (Lufaso, 2002, Galasso, 2013, Knapp, 2006). Double perovskite materials

took the attention of many researchers due to their interesting structural, magnetic and electrical properties. The general chemical formula of double perovskite oxides expressed as  $A_2BB'O_6$ , where A is Ca, Sr, Ba (one of the alkali elements of the first group or the second group in the

periodic table) and B site is occupied by first row of 3d magnetic element in the periodic table. The B' site is occupied by the 4d non-magnetic elements, with O atom located in between forming alternate BO<sub>6</sub> octahedral and B-O-B bonds oxygen atoms, The wide range of double perovskite material is due to alteration at the magnetic and non-magnetic of B and B' elements as well as the A-site cations (Yang *et al.*, 2015, Bharti *et al.*, 2014, Landinez Téllez *et al.*, 2014, Min *et al.*, 2012, Feraru *et al.*, 2013, Elbadawi *et al.*, 2013, Kim *et al.*, 2012b, Alsabah *et al.*, 2017b). The other chemical formula AA/BB/O<sub>6</sub> can be used as a different case where A, A' where occupied by rare elements such as Sr, Ca, Ba and La whereas B, B' occupied by transition metals such as Sr<sub>2</sub>FeMoO<sub>6</sub>, Sr<sub>2</sub>FeReO<sub>6</sub>, Sr<sub>2</sub>CrReO<sub>6</sub> and Sr<sub>2</sub>CoMoO<sub>6</sub> (Liu *et al.*, 2012, Retuerto *et al.*, 2015). The double perovskite material attracted the interest of researchers due to their wide range of the physical and application properties (Alsabah *et al.*, 2017). Some of double perovskite materials used as anode for the solid oxide fuel cells, optoelectronics, magnetic resonance (MIR), solar cells and microwave devices (Habisreutinger *et al.*, 2014). Here we refer to some important double perovskite studies for example, the La<sub>3</sub>Ni<sub>2</sub>NbO<sub>9</sub> and La<sub>3</sub>Ni<sub>2</sub>TaO<sub>9</sub> synthesized, both exhibited as monoclinic crystal structure using solid state preparation method and they used the XRD, SEM and the four-point probe technique as tools to describe the structure, morphology properties and the electrical conductivity of materials (Dey *et al.*, 2016). The effects in the crystal symmetry of (Sr<sub>x</sub>Ba<sub>1-x</sub>)CaW<sub>y</sub>Mo<sub>1-y</sub>O<sub>6</sub> doped Eu<sup>3+</sup> were studied by (Sletnes *et al.*, 2016). and they used the XRD, Raman spectroscopy to learn the effect of substitution in symmetry where the A-site was obtained as the main determinant for the crystal symmetry. The structure and magnetic properties of Ba<sub>2-x</sub>Sr<sub>x</sub>YIrO<sub>6</sub> series were investigated by (Phelan *et al.*, 2016). They used the XRD, high temperature measurement and Density functional theory (DFT) to characterize the material. The importance of this study depend on the use of the Doubleperovskite samples in the

solar cell fabrication because of their interaction with light. In general, the perovskite materials have increased the efficiency of solar cells and reduced the cost of manufacturing.

Photovoltaic (PV), also called solar cells, are electronic devices that convert sunlight directly into electricity. The modern form of the solar cell was invented in 1954 at Bell Telephone Laboratories. Today, PV is one of the fastest growing renewable energy technologies and it is expected that it will play a major role in the future global electricity generation mix (Neij, 1997). Perovskite solar cells have rapidly risen to the forefront of emerging photovoltaic technologies (Snaith *et al.*, 2014, Habisreutinger *et al.*, 2014), exhibiting externally verified power conversion efficiencies of over 16% (Snaith *et al.*, 2014). In order to use sunlight as efficiently as possible, low cost and efficient solar cells have been vigorously developed for practical use. As is generally known, practical silicon based solar cells involve high manufacturing cost, as well as any other inorganic based solar cells on the basis of the cost problem (Wang *et al.*, 2016). In this study we will use the X-ray diffraction, Uv.vis spectroscopy and IV curve characteristics to study the structure, optical properties and power conversion efficiencies of the CaLaFe<sub>1-x</sub>Mn<sub>x</sub>TiO<sub>6</sub> (x= 0, 0.67 and 0.33) double perovskite.



Double perovskite structure; The proposed double perovskite solar cell structure.

## Material and methods

New samples of double perovskite oxide were synthesized successfully using solid state interaction method by different treatments to get a single phase for the samples. The samples prepared by mixing stoichiometric amounts of all row material from Alfa Acer company of purity 99.9% that used to prepare the  $\text{CaLaMnTiO}_6$ ,  $\text{CaLaMn}_{0.67}\text{Fe}_{0.33}\text{TiO}_6$  and  $\text{CaLaMn}_{0.33}\text{Fe}_{0.67}\text{TiO}_6$  double perovskites oxides. The mixtures of compounds grinded in agate mortar with the addition of acetone then heated in air, after that the mixed was put in crucibles initially at  $800^\circ\text{C}$  during 12 hours, pellet in around shape and heated in  $1000^\circ\text{C}$ , finally it pelleted in around shape and heated in  $1100^\circ\text{C}$  two times permeated every grinding time with the addition of acetone. X-ray diffraction (XRD) data collected by a Bruker - axis D8 using  $\text{CuK}\alpha$  radiation ( $\lambda=1.54\text{\AA}$ ) at room temperature, with a nickel filter operating at 40 KV, 40 mA the data collected for the  $2\theta$  in 0.02 step size and five second count time in  $20^\circ - 80^\circ$  range. The Retvield method and the MDI jade program (Neij, 1997) were used for the XRD date analysis. The crystalline size (D) calculated by Scherer equation (Snaith, *et al.*, 2014, Neij, 1997) for the all samples.

$$D = \frac{0.94\lambda}{\beta_{1/2} \cos(\theta)} \quad (1)$$

Where D is crystallite size,  $\lambda$  is the wavelength of X-ray and  $\beta_{1/2}$  is the half-full width of the mean peaks (Thompson *et al.*, 1987, Holzwarth and Gibson, 2011).

A UV– visible spectrophotometer (Shimadzu, UV-2550) was used to calculate the UV– visible absorption spectrum at room temperature; the optical band gap energy was estimated using the onset of the absorption edge and by Taucs plot of the double perovskite samples according to the following equation.

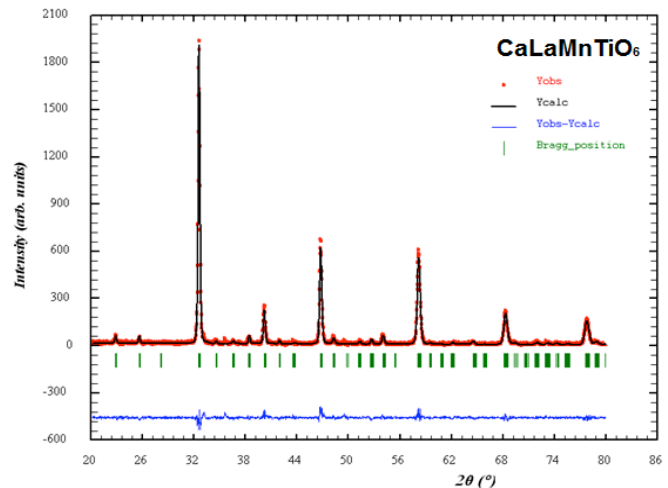
$$[F(R_{\infty})hv]^n = A(hv - E_g) \quad (2)$$

The three samples of double perovskite solar cells made by depositing double perovskite solution of fluorine doped tin oxide in FTO glass, and another layer made by depositing graphite particles on FTO glass. The fabrication process started by preparing the double perovskite materials and put them on FTO glasses. The FTO glasses were firstly cleaned by ethanol and distilled water. The double perovskites solution were deposited in FTO glasses, the glasses plate were put on the hot plate preheated to a temperature of the  $100^\circ\text{C}$ , when the film turned black, it was put on the Eriochrom-black T dye solution, then a small amount of graphite particles were put on the another FTO glass plate over it with the conductive side facing and sliding the two plates against each other. Being inserted electrical circuit containing (the voltmeter and Ammeter and a light source lamp with the intensity radiological and a solar cell) and stained using the procedure of H and E methods.

## Results and Discussion

### 3.1. Structural characterization

The XRD data of sample is shown in Figures (1, 2 and 3) for  $\text{CaLaMnTiO}_6$ ,  $\text{CaLaMn}_{0.67}\text{Fe}_{0.33}\text{TiO}_6$  and



$\text{CaLaMn}_{0.33}\text{Fe}_{0.67}\text{TiO}_6$ .

**Figure (1).** XRD refinement pattern of  $(\text{CaLaMnTiO}_6)$  double perovskite

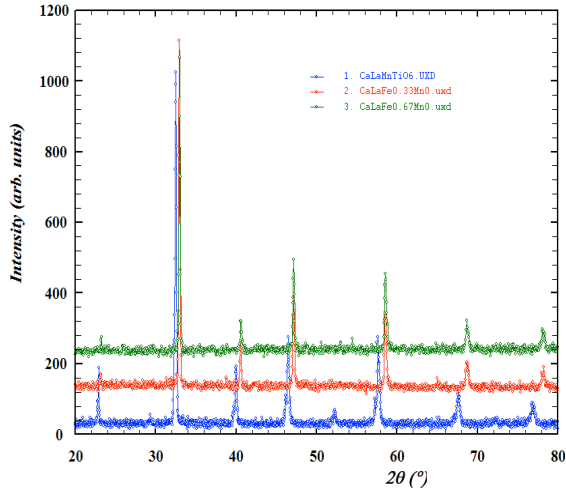


**Figure (2).** Shows XRD pattern comparison of CaLaMn1-xFexTiO6 (x= 0, 0.33 and 0.67) double perovskite.

The Retveld method and the fullprof program were used to analyze the XRD data of the samples. The CaLaMnTiO6 sample obtained a monoclinic structure with (P21/n) space group whereas the next samples obtained in (Pm-3m) 221 primitive cubic crystal structure, the lattice parameters found to be a =3.9471, 3.868Å for CaLaMn0.67Fe0.33TiO6 and CaLaMn0.33Fe0.67TiO6 respectively. The crystallite size calculated for the sample by Scherer equation for the samples. Table1 show the result of XRD analysis.

### 3.2. Optical characterization

The absorbance can be used to observe the absorption edge for the samples that shows in 255, 312 and 288 nm and the band gap was calculated from the absorption edge, that found to be 5, 4 and 3.6 eV for CaLaMnTiO6, CaLaMn0.67Fe0.33TiO6 and CaLaMn0.33Fe0.67TiO6 respectively. In addition, the band gap energy was calculated for samples by Tauc plot that shown in Figures (3-5) according to Eq. (2). Through the study of UV-visible absorption and optical energy gap of the sample classified as semiconductor materials. Table 1 shows the absorption edge and band gap energies of the series.

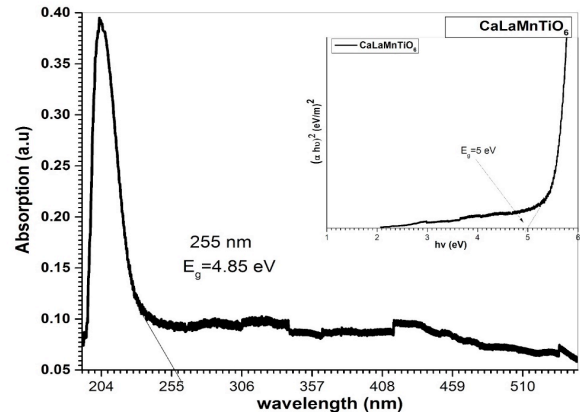


**Figure (3).** Shows absorption curve and Tauc plot of (CaLaMnTiO6) double perovskite.

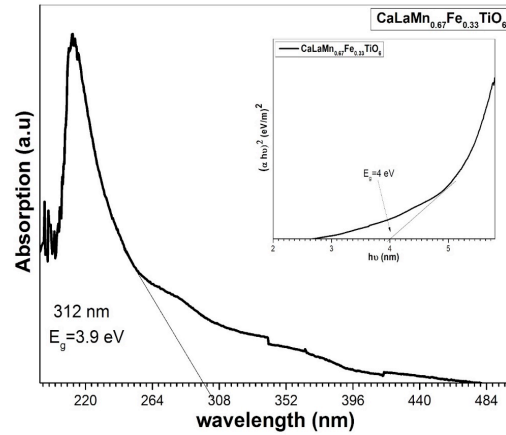


**Figure (4).** Absorption curve and Tauc plot of (CaLaMn0.67Fe0.33TiO6) double perovskite.

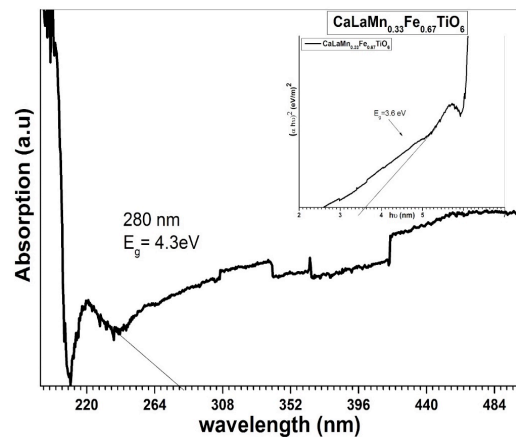


**Figure (5).** absorption curve and Tauc plot of (CaLaFe0.33Mn0.67TiO6) double perovskite.

Table (1): shows the absorption band bandgap energy of the series.

X ratio	CaLaMnTiO <sub>6</sub>	CaLaMn <sub>0.67</sub> Fe <sub>0.33</sub> TiO <sub>6</sub>	CaLaMn <sub>0.33</sub> Fe <sub>0.67</sub> TiO <sub>6</sub>
Cut-off wavelength (nm)	255	312	280
E <sub>g</sub> (eV) by cutoff wavelength	4.85	3.9	4.3
E <sub>g</sub> (eV) by Tauc plot	5	4	3.6

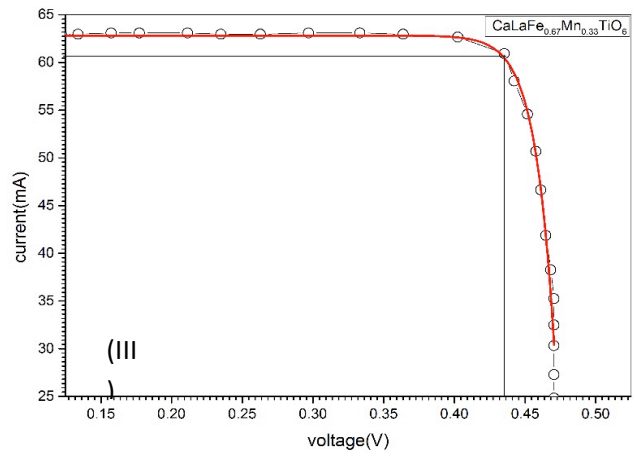


Figure 6 (I-III) Curve of CaLaMn<sub>1-x</sub>Fe<sub>x</sub>TiO<sub>6</sub>(x= 0, 0.33 and 0.67) double perovskite of Solar Cell.

### 3.3 I-V characteristic

The current voltage (I-V) readings for the double perovskite solar cell samples are enumerated in the table (2). I-V results were displayed graphically in Figure 6 (I-III).

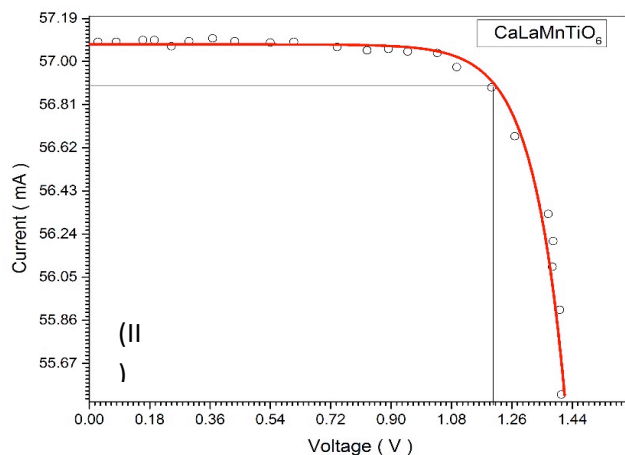
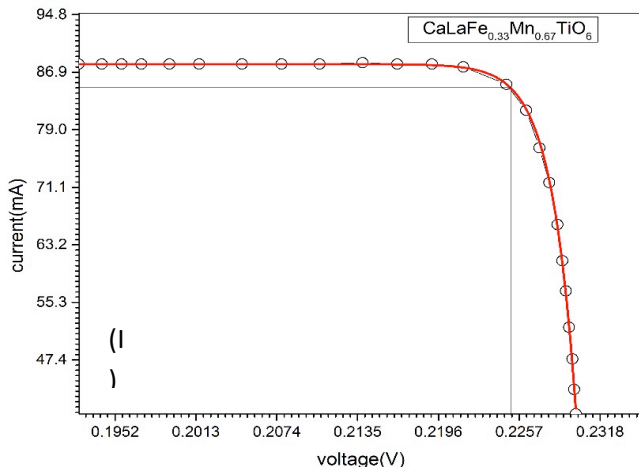


Table (2): shows XRD result.

samples	CaLaMnTiO <sub>6</sub>	CaLaMn <sub>0.67</sub> Fe <sub>0.33</sub> TiO <sub>6</sub>	CaLaMn <sub>0.33</sub> Fe <sub>0.67</sub> TiO <sub>6</sub>
Space group	monoclinic (P21/n)	(Pm-3m)Cubic	(Pm-3m)Cubic
a , b , c	a =5.47953 Å b = 5.54992 Å c = 7.76430 Å	3.974 Å	3.868 Å
α = β = γ	90	90	90
Unite cell volume	236.11 Å <sup>3</sup>	61.49 Å <sup>3</sup>	57.85 Å <sup>3</sup>
Crystallite size (nm)	43.18	60.83	45.06
Lattice strain	0.0030	0.0022	0.0028

The figures are used to find I<sub>sc</sub> (short circuit current), V<sub>oc</sub>(open circuit voltage), I<sub>max</sub> (maximum current) and V<sub>max</sub> (maximum voltage). It was found that those parameters had the J<sub>sc</sub> of samples (J<sub>sc</sub>=I<sub>sc</sub>/Area), and where the fill factor (FF) was got by dividing maximum out power (P<sub>max</sub>) by the product of short-circuit current and the open-circuit voltage FF=(I<sub>max</sub>\*V<sub>max</sub>)/(I<sub>sc</sub>\*V<sub>oc</sub>)[5]. The maximum power was given by max volt V<sub>max</sub> and max current I<sub>max</sub>. The power conversion efficiency η of the double perovskite solar cell is determined by the

photocurrent density asured at short-circuit  $V_{oc}$ , the FF of the cell, and the open-circuit and  $J_{sc}$  (Kim *et al.*, 2012a, Li *et al.*, 2010).

$$\eta = (J_{sc} * V_{oc} * FF) / P_{in} [5]$$

These results for the three samples were recorded in Table (3). The variation in efficiency for the three samples is often due to the doping rates.

Table (3): shows the basis electrical properties of the

Sample	Area (cm <sup>2</sup> )	$J_{sc}$ (mA)	$V_{oc}$ (V)	$J_{sc}$ (mA/cm <sup>2</sup> )	FF	PCE(%)
CaLaMnTiO <sub>6</sub>	5.76	57.1	1.42	9.91	0.84	1.18
CaLaMn <sub>0.67</sub> Fe <sub>0.33</sub> TiO <sub>6</sub>	6.21	62.94	0.47	10.12	0.89	0.42
CaLaMn <sub>0.33</sub> Fe <sub>0.67</sub> TiO <sub>6</sub>	6	87.62	0.230	14.6	0.95	0.32

proposed perovskite solar cells

#### 4. Conclusion

The double perovskite oxide with formula CaLaMn<sub>1-x</sub>Fe<sub>x</sub>TiO<sub>6</sub> where (x= 1, 0.33, 0.67) was successfully prepared. The samples show variation in crystal structure from monoclinic to cubic. The band gap of the samples from the absorption edge were found to be closer to the value that calculated by Tauc plot. The absorption and optical band gap energy classified the series as semiconductor materials. Double Perovskite solar cell based on a Thin Film Double Perovskite active layer of solar cell sandwiched between FTO and graphite on FTO electrodes were fabricated. The three FTO, double perovskite and graphite of FTO solar cells were produced and characterized, which provided  $\eta$  of (1.18, 0.42, and 0.32%), FF of (0.84, 0.89, and 0.95),  $J_{sc}$  of (9.91, 10.12, and 14.6

mA/cm<sup>2</sup>) and  $V_{oc}$  of (1.42, 0.47, and 0.230V). It is clear that the variation in the structure, decreasing in energy band gap and solar cell efficiency may due to the increasing of iron dopant on the B/ site of the CaLaMn<sub>1-x</sub>Fe<sub>x</sub>TiO<sub>6</sub>(x= 0, 0.33 and 0.67) double perovskite. Formation of Double Perovskite active layer with homogeneously distributed Double Perovskite nano-wires would have been improving the efficiencies of the solar cells. To increase power conversion efficiency, structures of the solar cells should be optimized.

The double perovskite oxide with formula CaLaMn<sub>1-x</sub>Fe<sub>x</sub>TiO<sub>6</sub> where (x= 1, 0.33, 0.67) was successfully prepared. The samples show variation in crystal structure from monoclinic to cubic. The band gap of the samples from the absorption edge were found to be closer to the value that calculated by Tauc plot. The absorption and optical band gap energy classified the series as semiconductor materials. Double Perovskite solar cell based on a Thin Film Double Perovskite active layer of solar cell sandwiched between FTO and graphite on FTO electrodes were fabricated. The three FTO, double perovskite and graphite of FTO solar cells were produced and characterized, which provided  $\eta$  of (1.18, 0.42, and 0.32%), FF of (0.84, 0.89, and 0.95),  $J_{sc}$  of (9.91, 10.12, and 14.6 mA/cm<sup>2</sup>) and  $V_{oc}$  of (1.42, 0.47, and 0.230V). It is clearly that the variation in the structure, decreasing in energy band gap and solar cell efficiency may due to the increasing of iron dopant on the B/ site of the CaLaMn<sub>1-x</sub>Fe<sub>x</sub>TiO<sub>6</sub>(x= 0, 0.33 and 0.67) double perovskite. Formation of Double Perovskite active layer with homogeneously distributed Double Perovskite nano-wires would have been improving the efficiencies of the solar cells. To increase power conversion efficiency, structures of the solar cells should be optimized.

## References

- Alsabah, Y. A., Alsahhi, M. S., Elbadawi, A. A. & Mustafa, E. M. (2017). Influence of Zn<sup>2+</sup> and Ni<sup>2+</sup> cations on the structural and optical properties of Ba<sub>2</sub>Zn<sub>1-x</sub>Ni<sub>x</sub>WO<sub>6</sub> (0 ≤ x ≤ 1) tungsten double perovskites. *Journal of Alloys and Compounds*, 701, 797-805.
- Bharti C, Das MK, Sen A, Chanda S, Sinha T. (2014). Rietveld refinement and dielectric relaxation of a new rare earth based double perovskite oxide: BaPrCoNbO<sub>6</sub>. *Journal of Solid State Chemistry*; 210(1):219-23.
- Dey, K., Indra, A., DE, D., Majumar, S. & Giri, S. (2016). Magnetoelectric coupling, ferroelectricity, and magnetic memory effect in double perovskite La<sub>3</sub>Ni<sub>2</sub>NbO<sub>9</sub>. *ACS applied materials & interfaces*, 8, 12901-12907.
- ELBadawi., A. A., Yassin, O. A. & Gismelseed, A. A. (2013). Effect of the internal pressure and the anti-site disorder on the structure and magnetic properties of ALaFeTiO<sub>6</sub> (A=Ca, Sr, Ba) double perovskite oxides. *Journal of Magnetism and Magnetic Materials*, 326, 1-6.
- Feraru S, Samoila P, Borhan A, Ignat M, Iordan A, Palamaru M. (2013). Synthesis, characterization of double perovskite Ca<sub>2</sub>MSbO<sub>6</sub> (M= Dy, Fe, Cr, Al) materials via sol-gel auto-combustion and their catalytic properties. *Materials Characterization*. 84, 112-9.
- Gallasso, F. S. (2013). *Structure, Properties and Preparation of Perovskite-Type Compounds: International Series of Monographs in Solid State Physics*, Elsevier.
- Habisreuinger, S. N., Leijtens, T., Eperon, G. E., Stranks, S. D., Nicholas, R. J. & Snaith, H. J. (2014). Carbon nanotube/polymer composites as a highly stable hole collection layer in perovskite solar cells. *Nano letters*, 14, 5561-5568.
- Holzwarth, U. & Gibson, N. (2011). The Scherrer equation versus the 'Debye-Scherrer equation'. *Nature Nanotechnology*, 6, 534.
- Kim H.-S., Lee, C.-R., IM, J.-H., Lee, K.-B., Moehl, T., Marchioro, A., Moon, S.-J., Humphery-Baker, R., Yum, J.-H. & Moser, J. E. (2012a). Lead iodide perovskite sensitized all-solid-state submicron thin film mesoscopic solar cell with efficiency exceeding 9%. *Scientific reports*, 2, 591.
- Kim, H.-S., Lee, C.-R., IM, J.-H., Lee, K.-B., Moehi, T., Marchioro, A., Moon, S.-J., Humphery-Baker, R., YUM, J.-H., Moser, J. E., Gratzel, M. and Park, N.-G. 2012b. Lead Iodide Perovskite Sensitized All-Solid-State Submicron Thin Film Mesoscopic Solar Cell with Efficiency Exceeding 9%. *Scientific Reports*, 2, 591.
- Knapp, M. C. (2006). Investigations into the structure and properties of ordered perovskites, layered provskites and defect pyrochlores. The Ohio State University.
- Landinez T., D. A., Martinez , Buttrago, D., Cardona C, R., Barrera, E. W. & Roa-Rojas, J. (2014). *Journal of Molecular Structure*, 1067, 205-209.
- Li, L., Gipson, E. A., QIN, P., BOSCHLOO, G., GORLOV, M., Hagfldt, A. & Sun, L. (2010). Double Layered NiO Photocathodes for p-Type DSSCs with Record IPCE. *Advanced Materials*, 22, 1759-1762.
- Lufaso M. W. (2002). Perovskite synthesis and analysis using structure prediction diagnostic software: The Ohio State University;.
- Min L, Hong-ming Y, Wei X., Mei H., Lin-ran Y., Ming Y, (2012). Hydrothermal Synthesis and Dielectric Characterization of a Double Perovskite Ba<sub>2</sub>FeSbO<sub>6</sub>. *Chemical Research in Chinese Universities*. 28(5):788-91.
- Neij L. (1997). Use of experience curves to analyse the prospects for diffusion and adoption of renewable energy technology. *Energy policy* 25(13):1099-107.
- Snaith H. J, Abate A, Ball JM, Eperon GE, Leijtens T, Noel NK, et al. Anomalous hysteresis in perovskite solar cells. *The Journal of Physical Chemistry Letters*. 2014;5(9):1511-5.
- Wang D-L, Cui H-J, Hou G-J, Zhu Z-G, Yan Q-B, Su G. Highly efficient light management for perovskite solar cells. *Scientific Reports*. 2016;6.
- Yang, . S, Yan N, Chenl S, Zhang Y. (2015). Structural and optical properties of BiFeO<sub>3</sub> system multiferroic films prepared by sol-gel method. *Ceramics International*.